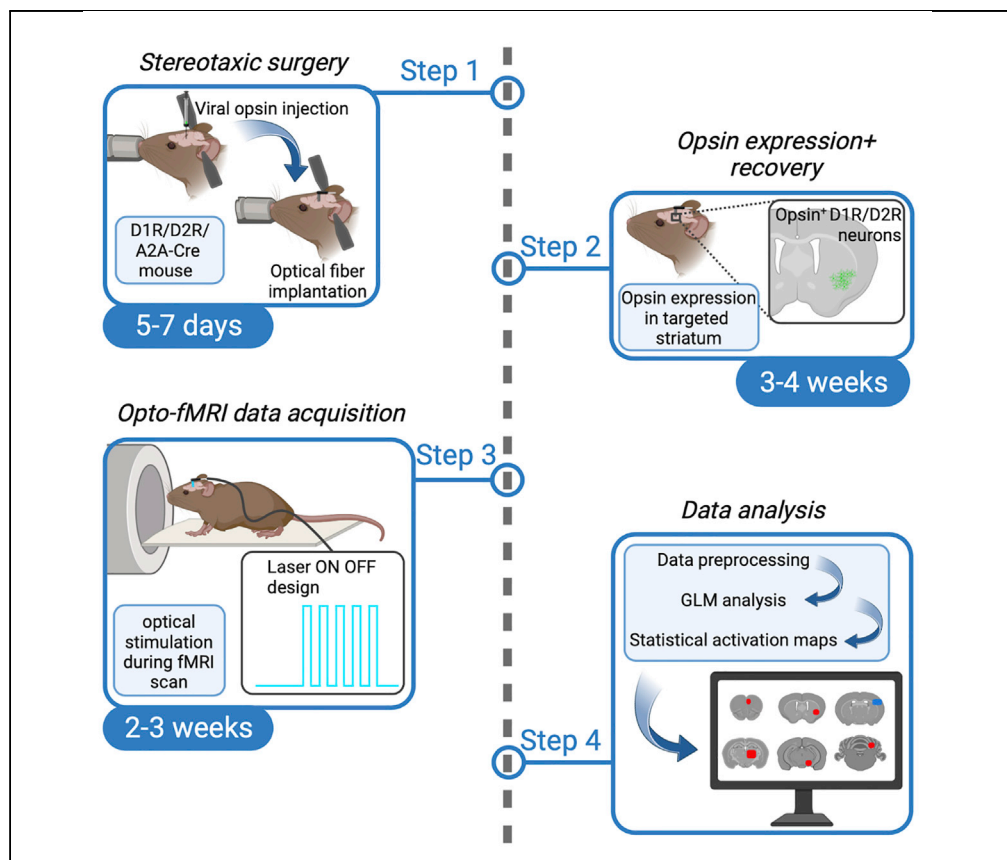


## Protocol

# An optimized protocol for assessing changes in mouse whole-brain activity using opto-fMRI



Christina Grimm,  
Nicole Wenderoth,  
Valerio Zerbi

christina.grimm@epfl.ch  
(C.G.)  
valerio.zerbi@epfl.ch  
(V.Z.)

### Highlights

Step-by-step instructions to perform opto-fMRI in mice

Guidelines for fMRI-compatible optical implants

Measurement of whole-brain BOLD fMRI during optogenetic stimulation

Pre-processing and analysis of functional opto-fMRI datasets

Functional magnetic resonance imaging (fMRI) in mouse brain, paired with spatially and temporally defined manipulations, offers a powerful tool to causally explain the effect of specific neuronal activity on brain network dynamics. Here, we present an optimized protocol to measure cell-type-specific contributions to changes in whole-brain dynamics in mice using optogenetics (opto)-fMRI. This protocol details the injection of ChR2-expressing AAV, the implantation of optical fiber, the steps to perform opto-BOLD (blood-oxygenation-level-dependent) fMRI recording, and data analysis.

Publisher's note: Undertaking any experimental protocol requires adherence to local institutional guidelines for laboratory safety and ethics.

Grimm et al., STAR Protocols  
3, 101761  
December 16, 2022 © 2022  
The Author(s).  
<https://doi.org/10.1016/j.xpro.2022.101761>



## Protocol

## An optimized protocol for assessing changes in mouse whole-brain activity using opto-fMRI

Christina Grimm,<sup>1,2,3,4,5,\*</sup> Nicole Wenderoth,<sup>1,2</sup> and Valerio Zerbi<sup>1,2,3,4,6,\*</sup><sup>1</sup>Neural Control of Movement Lab, Department of Health Sciences and Technology (D-HEST), ETH Zurich, 8092 Zurich, Switzerland<sup>2</sup>Neuroscience Center Zurich, ETH Zurich and University of Zurich, 8057 Zurich, Switzerland<sup>3</sup>Neuro-X Institute, School of Engineering (STI), EPFL, 1015 Lausanne, Switzerland<sup>4</sup>CIBM Center for Biomedical Imaging, 1015 Lausanne, Switzerland<sup>5</sup>Technical contact<sup>6</sup>Lead contact\*Correspondence: [christina.grimm@epfl.ch](mailto:christina.grimm@epfl.ch) (C.G.), [valerio.zerbi@epfl.ch](mailto:valerio.zerbi@epfl.ch) (V.Z.)  
<https://doi.org/10.1016/j.xpro.2022.101761>

## SUMMARY

Functional magnetic resonance imaging (fMRI) in mouse brain, paired with spatially and temporally defined manipulations, offers a powerful tool to causally explain the effect of specific neuronal activity on brain network dynamics. Here, we present an optimized protocol to measure cell-type-specific contributions to changes in whole-brain dynamics in mice using optogenetics (opto)-fMRI. This protocol details the injection of Chr2-expressing AAV, the implantation of optical fiber, the steps to perform opto-BOLD (blood-oxygenation-level-dependent) fMRI recording, and data analysis.

For complete details on the use and execution of this protocol, please refer to Grimm et al. (2021).

## BEFORE YOU BEGIN

The protocol below describes the specific steps in *Drd1-Cre*, *Drd2-Cre*, and *A2A-Cre* mouse lines, with optogenetic targeting of striatal D1 and D2 receptor cells. Subsequently, it provides detailed instructions on how to conduct fMRI recordings combined with optogenetic stimulation of striatal D1 and D2 receptor cells in the mouse *Cre*-lines. Ideally, proper titration of the viral construct as well as correct targeting of the brain region in question should be confirmed in a sub-set of mice prior to the experimental study. To yield the most reliable study results all animals should be around the same age (8–12 weeks) at the time of data collection. All experimental steps involving laboratory animals must conform to the institutional guidelines for the care and use of laboratory animals. The experimental procedures for fMRI recordings described here have been employed in a number of earlier research conducted in our lab that centered on mouse resting-state brain activity (Grandjean et al., 2020; Zerbi et al., 2015, 2018, 2019b) and multi-modal fMRI acquisitions achieved by chemogenetic manipulations (Markicevic et al., 2020; Zerbi et al., 2019a). More recently, we have also used this protocol to acquire fMRI recordings during optogenetic stimulation of noradrenergic neurons in the locus coeruleus of *DBH-iCre* mice (Grimm et al., 2022).

## Institutional permissions

All animal procedures were conducted in accordance with the Swiss Federal Ordinance on Animal Experimentation and approved by the Cantonal Veterinary Office of Zurich.



**KEY RESOURCES TABLE**

REAGENT or RESOURCE	SOURCE	IDENTIFIER
<b>Bacterial and virus strains</b>		
AAV-5/2-hEF1 $\alpha$ -dlox-hChR2(H134R)_EYFP(rev)-dlox-WPRE-hGHp(A)	Viral Vector Facility (VVF), Switzerland	VVF Repository: v214-5
AAV-5/2-hSyn-dlox-EYFP(rev)-dlox-WPRE-hGHp(A)	Viral Vector Facility (VVF), Switzerland	VVF Repository: V115-5
<b>Chemicals, peptides, and recombinant proteins</b>		
Pancuronium bromide	Sigma-Aldrich, USA	Cat#P1918
Isoflurane (Attane)	Piramal Healthcare Limited, India	Swissmedic #56761
Midazolam (Benzodiazepine)	Neuraxpharm Switzerland AG, Switzerland	Swissmedic #62556
Medetomidine (Imidazole)	Orion Pharma, Finland	Swissmedic #50590
Fentanyl	Sintetica SA, Switzerland	Swissmedic #53987
Temgesic (Buprenorphine)	Indivior Schweiz AG, Switzerland	Swissmedic #41931
Antisedan (Atipamezole)	Orion Pharma, Finland	Swissmedic #50819
Anexate (Flumazenil)	CPS Cito Pharma Services GmbH, Switzerland	Swissmedic #48280
0.9% NaCl (Saline)	B. Braun Melsungen AG, Germany	Item Number: 3570310
Permaplast LH Flow, dental cement	M+W Dental, Switzerland	Item Number: 100105
Etching gel	DMG, Germany	Cat #198178
OptiBond All in one, dental bonding agent	Kerr Dental, Germany	Item Number: 33533
Lacrinorm gel opht, eye protectant gel	Bausch+Lomb Swiss AG	Pharmacode: 7570255
Non-absorbable, silk suture material (3/0 met, HS15, 45 cm)	B. Braun Melsungen AG, Germany	Item Number: G0762059
<b>Deposited data</b>		
Mouse brain template	Allen Institute (Oh et al., 2014)	RRID:SCR013286; <a href="http://mouse.brain-map.org/static/atlas">http://mouse.brain-map.org/static/atlas</a>
Mouse GE-BOLD datasets	(Grimm et al., 2021)	zenodo.org <a href="https://doi.org/10.5281/zenodo.6770220">https://doi.org/10.5281/zenodo.6770220</a> .
Mouse anatomical datasets	(Grimm et al., 2021)	zenodo.org <a href="https://doi.org/10.5281/zenodo.6770220">https://doi.org/10.5281/zenodo.6770220</a> .
<b>Experimental models: Organisms/strains</b>		
Mouse Cre-line: B6.FVB(Cg)-Tg(Drd1-cre)EY262Gsat/Mmucd; age: 8–12 weeks; sex: male and female	(Gong et al., 2007)	MGI:3836631
Mouse Cre-line: B6.FVB(Cg)-Tg(Drd2-cre)ER44Gsat/Mmucd; age: 8–12 weeks, sex: male and female	(Gong et al., 2007)	MGI:3836635
Mouse Cre-line: B6.FVB(Cg)-Tg(Adora2a-cre)KG139Gsat/Mmucd; age: 8–12 weeks; sex: male and female	(Gong et al., 2007); Laboratory of Prof. Denis Burdakov	MGI:4361654
<b>Software and algorithms</b>		
MATLAB	MathWorks	RRID:SCR_001622; <a href="https://matlab.mathworks.com">https://matlab.mathworks.com</a>
FSL	Analysis Group, FMRIB, Oxford, UK	RRID:SCR_002823; <a href="https://fsl.fmrib.ox.ac.uk/fsl/downloads_registration">https://fsl.fmrib.ox.ac.uk/fsl/downloads_registration</a>
ANTS (Advanced Normalization Tools)	(Avants et al., 2010, 2011)	RRID:SCR_004757; <a href="http://picsl.upenn.edu/software/ants/">http://picsl.upenn.edu/software/ants/</a>
TAPAS	(Frässle et al., 2021)	<a href="https://www.tnu.ethz.ch/de/software/tapas">https://www.tnu.ethz.ch/de/software/tapas</a>
COSplay trigger	(Aymanns et al., 2020)	<a href="https://cosplay.readthedocs.io/en/latest/">https://cosplay.readthedocs.io/en/latest/</a>
<b>Other</b>		
Stereotaxic frame	Neurostar, Germany	N/A
Dental drill and drill bit	Neurostar, Germany	N/A
Dental scaler	M+W Dental, Switzerland	Item number: 140610
Bruker PharmaScan 7T	Bruker Corporation, USA	N/A
Cryogenic coil	Bruker Corporation, USA	N/A
MRI-compatible small animal cradle	Bruker Corporation, USA	N/A

(Continued on next page)

### Continued

REAGENT or RESOURCE	SOURCE	IDENTIFIER
MRI-compatible heating system (LAUDA Eco E4 Silver)	LAUDA, Germany	Item number: LAU_16006
Temperature probe (Optocon Fotemp4)	Optocon by Weidmann, Germany	N/A
MRI-compatible LED lamp	N/A	N/A
MRI-compatible small animal ventilator	CWE Incorporated, USA	Part Number: 12-07000
MRI-compatible small animal injectomat (Standard Infuse/Withdraw PHD ULTRA™ Syringe Pump)	Harvard Apparatus, USA	Item number: 70-3007
Low-profile cannula holder	Doric Lenses, Canada	Ordering code: SCH-LP90
Custom-made, low profile optical fiber cannula	Doric Lenses, Canada	Ordering code: MFC_mm_LPB90(P)_FLT
Custom-made, MRI-compatible fiber patch cable	Thorlabs, Germany	Part number: FT200EMT-custom
Phosphor bronze mating sleeve	Thorlabs, Germany	Item number prefix: ADAL4
Wireless, handheld power meter	Thorlabs, Germany	Item number: PM160
Laser safety goggles	Thorlabs, Germany	Item number: LG3
Custom-made, 3-wavelength laser (635/532/473 nm)	CNI laser, China	Model: MSIII-W-635/532/473/1–500mW
Customized laser (473 nm)	N/A	N/A
Endotracheal intubation tubing	Multi Channel Systems MCS GmbH, Germany	Item Number: 640752
Tail vein cannulation tubing	Multi Channel Systems MCS GmbH, Germany	Item Number: 640751
Insulin syringe, 1 mL	Braun, USA	Omnican 100; Product Code: 9151141
2-piece fine dosage syringe, 1 mL	Braun, USA	Inject-F solo; Product Code: 9166017V
Single-use hypodermic insulin needle	Braun, USA	Sterican; Product Code: 4657519
Disposable dental needle, 25G	Braun, USA	Cat #: 6.510 863
Disposable dental needle, 30G	WM Supplies, BEL	Item Number: 605303
Heating pad	Harvard Apparatus, USA	Item Number: 72-0494
Heating chamber	Peco Services, UK	Item Number: V1200

## MATERIALS AND EQUIPMENT

### Anesthesia reagents for stereotaxic surgery

Reagent	Dosage	Amount
Midazolam	5 mg/kg	N/A
Medetomidine	0.05 mg/kg	N/A
Fentanyl	0.05 mg/kg	N/A

For injection of the anesthetic reagents always weigh the animal. Each injection volume needs to be adapted individually according to the body weight. Store reagents in a dark space at room temperature (20°C–23°C) and respect expiration dates of individual reagents.

### Anesthesia antidote reagents for stereotaxic surgery

Reagent	Dosage	Amount
Atipamezole	2.5 mg/kg	N/A
Buprenorphine	0.1 mg/kg	N/A
Flumazenil	0.5 mg/kg	N/A

For injection of the anesthesia antidote reagents always weigh the animal. Each injection volume needs to be adapted individually according to the body weight. Store reagents in a dark space at room temperature (20°C–23°C) and respect expiration dates of individual reagents.

**Alternatives:** This protocol uses several anesthetic and anesthesia-reversing reagents for stereotaxic surgery. Alternatively, stereotaxic procedures can be performed under isoflurane paired with a systemically and locally applied analgesic.

### Anesthesia reagents for opto-fMRI recording

Reagent	Dosage	Amount
Pancuronium bromide	0.25 mg/kg	N/A
Medetomidine	0.05 mg/kg	N/A

For injection of the anesthetic reagents always weigh the animal. Each injection volume needs to be adapted individually according to the body weight and may be mixed in NaCl (0.9%). Store reagents in a dark space at room temperature (20°C–23°C) and respect expiration dates of individual reagents.

**Alternatives:** This protocol uses the MRI-compatible dental cement Permaplast LH Flow. An alternative MRI-compatible dental cement is the Scotchbond Universal adhesive (3M, Switzerland), which similarly creates minimal artifacts.

**Alternatives:** This protocol uses custom-made, low profile optical fiber cannulas, optimized to fit an MRI cryogenic coil set-up. When using a standard MRI surface coil, generic MRI-compatible fiber-optic cannulas can be implanted instead.

## STEP-BY-STEP METHOD DETAILS

### Stereotaxic surgery

⌚ **Timing:** 1–1.5 h for stereotaxic surgery

Mice are stereotaxically injected with an AAV construct to express the optogenetic actuator ChR2 in the target region and implanted with a low-profile, small-bore MRI-compatible optic cannula.

1. Prepare animal for stereotaxic surgery.
  - a. Induce anesthesia for stereotaxic surgery in a dedicated chamber using 4% isoflurane in a 1:4 O<sub>2</sub> to air mixture.
  - b. Weigh the animal and prepare anesthesia mixture according to the weight.
  - c. Inject anesthesia mixture intramuscularly into the quadriceps femoris muscle.
  - d. Generously shave hair from the neck up to the front of the eyes.
  - e. Apply epilation cream to the shaved head and let sit for 1 min. Remove with a lint-free cloth.
2. Secure the animal in the stereotaxic frame, placed on top of a heating pad maintained at ~36°C.
  - a. Cover eyes with an artificial tear ointment to avoid drying of eyes.
  - b. Inject lidocaine (20–50 µL) under the scalp to prevent pain.
3. Cut a large oval section of the scalp to expose the skull using sterile forceps and scissors.
  - a. Remove all tissue covering the skull using sterile cotton buds. Avoid damage to the muscles.
  - b. Clamp the surrounding skin with spring scissors to evenly expose anterior, posterior, and parietal areas of the skull.
4. Apply a thin layer of dental etching gel to the exposed skull while avoiding contact with soft tissue. Let sit for 30 s before removing it with sterile cotton buds.
  - a. Carefully scrape the bone surface of the animal's skull with a dental scraper in a horizontal, vertical, and diagonal way to create ridges for the dental cement to adhere to (Figure 1).
  - b. Wash off bone debris with saline and dry the skull using lint-free, medical-grade sponge material. Do not desiccate.
5. Locate bregma and lambda positions and correct for tilt and scaling accordingly.
6. Navigate to the desired coordinates (AP -0.1; ML -2.6; DV 3.7, relative to bregma).
  - a. Carefully start drilling a small hole using a dental drill (30'000 rpm), without severing the cortical surface.
  - b. Remove any bone debris from the skull using a rubber air puffer.

⚠ **CRITICAL:** Clean any bloody tissue surrounding the drill hole using saline and lint-free, medical-grade sponge material. Any trapped and clotted blood will result in MR signal

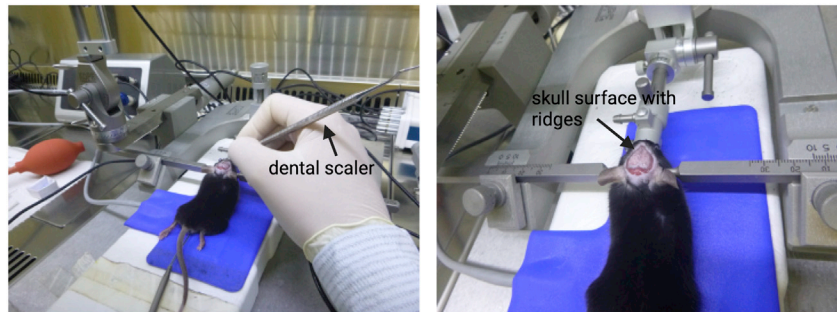


**Figure 1. Skull surface preparation**

Using a dental scaler, horizontal, vertical, and diagonal ridges are scraped on the skull surface. The resulting bone debris is removed using saline and lint-free sponge material.

loss due to the paramagnetic properties of deoxyhemoglobin. After cleaning, keep any exposed brain tissue submerged in sterile saline.

7. Perform viral injection.
8. Let the injection needle sit in place for ~5–10 min (depending on injected volume) to avoid any fluid drawback during needle retraction.

△ **CRITICAL:** Stop any bleeding that may occur during needle retraction with medical-grade sponge material before optical fiber implantation. This will ensure no additional MR artifacts due to clotted blood surrounding the optical fiber. Keep exposed tissue submerged in sterile saline.

9. Place optical fiber in stereotactic holder and lower it toward the cortical surface.
10. Slowly (~1200  $\mu\text{m}/\text{min}$ ) drive the optical fiber into the brain tissue, making sure no bleeding occurs.
11. Once the optical fiber is in place, dry the skull using a rubber air puffer. Do not desiccate.
12. Apply a thin layer of bonding agent to the exposed skull and light-cure for 20 s with a dental curing light.

△ **CRITICAL:** Steer clear of the optical implant and drill hole as the reagent has an acidic pH that will damage both the optical fiber and brain tissue, resulting in substantial MR artifacts.

13. Apply the dental composite Permaplast LH flow and light-cure it for 20 s. Start at the plastic edges of the optical fiber and build up in layers. This will embed the optical implant and contribute to its longevity.
  - a. Once the optical implant is secure, remove the stereotaxic holder.
  - b. Apply the dental composite in layers to the remaining exposed skull and light cure each layer for 20 s.

△ **CRITICAL:** Avoid introducing air bubbles while building the dental composite layers as this will create MR artifacts. This can be easily avoided by handling the dental cement syringe in a gentle manner (i.e., no shaking) and removing any bubbles forming at the tip of the syringe using a tissue. Keep the total dental composite layer to the height of the optical implant.

14. Apply non-absorbable silk stitches to the anterior and posterior skin flaps as needed.
15. Subcutaneously inject the anesthesia antidote and 100  $\mu\text{L}$  of Saline to rehydrate mice. Put them in a heating chamber for recovery.



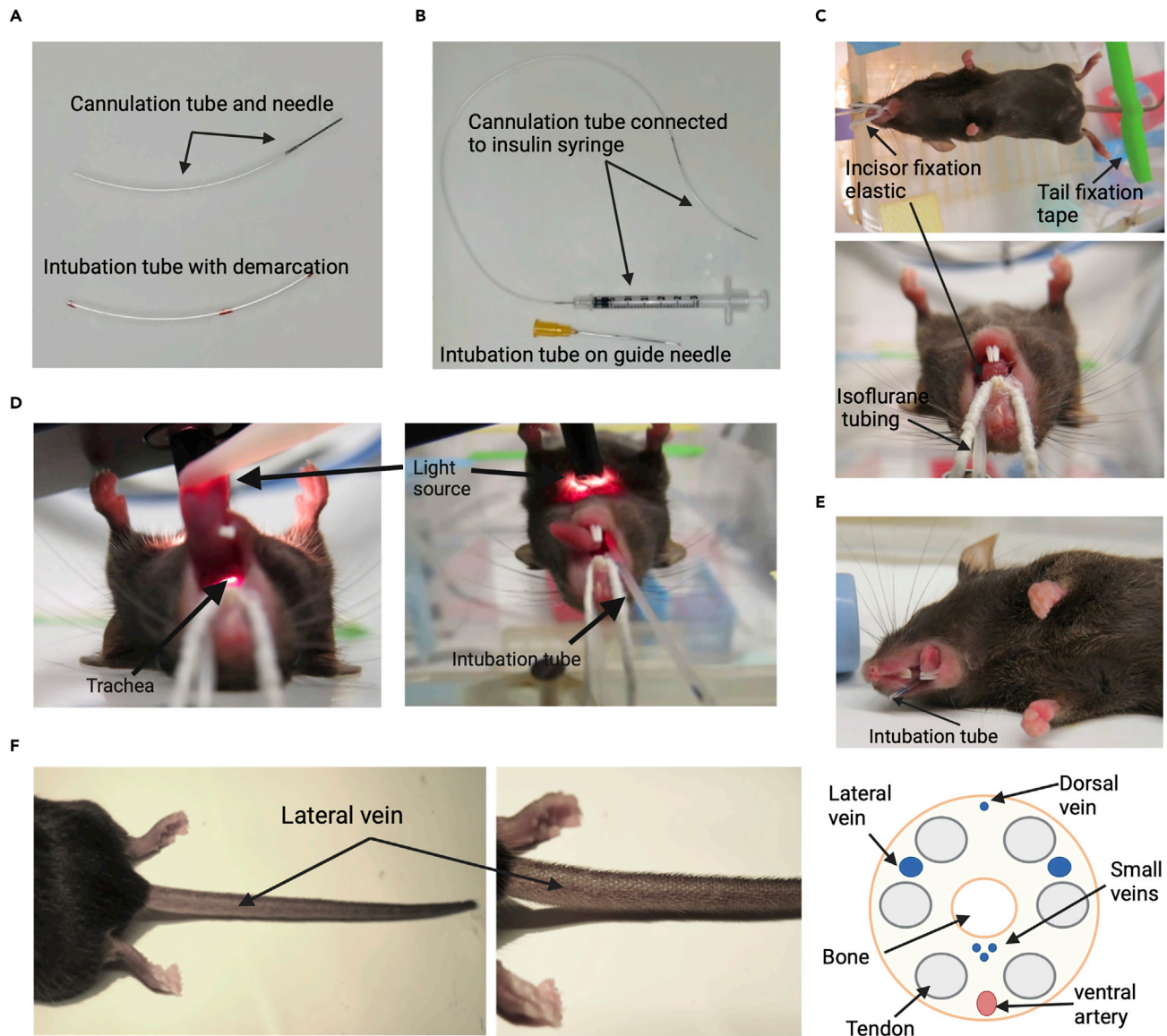


**Figure 2. Endotracheal intubation and tail vein cannulation procedure for opto-fMRI recordings in the anesthetized state**

(A) Cannulation and intubation tubing 4 cm. Insert a 30G needle tip into the cannulation tube.

(B) Connect the cannulation tube to an insulin syringe filled with sterile saline via a longer tube connected to a 30G needle and pre-fill tubings and needles with sterile saline. Slide intubation tube onto a 25G needle tip for guide purposes.

(C) Place the anesthetized mouse onto a platform facing belly up and secure front incisors with an elastic. Tape the tail to the platform surface for additional stability and position an isoflurane tubing along the buccal tissue inside the mouth to maintain anesthesia.

(D) Place a light source above the animal's neck to visualize the trachea. Once located, intubate the mouse using the guided intubation tube.

(E) Once the mouse is successfully intubated, a faint rhythmic condensation pattern should be visible inside the intubation tube. Cut the tube at the demarcation line creating a bevel.

(F) Position the intubated mouse on a heating pad, reducing isoflurane anesthesia to 2%. Locate the lateral tail vein and cannulate the animal. Once successfully cannulated, blood should easily be drawn from and re-injected into the tail vein using the insulin syringe connected to the cannulation tubing.

### Opto-fMRI recording

© Timing: 10–15 min for animal preparation, 1 h for opto-fMRI recordings

Combined optogenetic stimulation and fMRI recordings in mice capture cell-type specific contributions to changes in brain-wide activity.

16. Slide a 4 cm intubation tube with a demarcation at 2.5 cm onto a 25 gauge needle tip and prepare a 4 cm cannulation tube connected to a 30 gauge needle tip. Connect the cannulation tube to a separate, longer tubing attached to a 1 mL insulin syringe filled with sterile saline (Figures 2A and 2B).
17. Anesthetize the mouse in a separate chamber with 4% isoflurane (1:4 O<sub>2</sub> to air mixture) for 4 min.
18. Position the animal on an elevated platform facing belly up once the timer has expired.
  - a. Secure upper incisors in an elastic hoop to overextend the neck.
  - b. Tape the tail to the platform surface using adhesive tape (Figure 2C).
  - c. Maintain anesthesia at 4% isoflurane flow through redirected tubing placed inside the animal's mouth (Figure 2C).
  - d. Put a small heating pad (~36°C) on top of the tail to maintain a stable core temperature.
19. Position a light source above the animal's neck to readily locate the trachea (Figure 2D).
  - a. Perform endotracheal intubation with the dedicated, 4 cm long tube (Figure 2D). For an instructive videographic documentation of the intubation process please see (Das et al., 2013).
  - b. Cut the tube at the demarcation, creating a bevel (Figure 2E).
  - c. Transfer the animal to a heating pad and reduce the isoflurane flow to 2%.
  - d. Cannulate the lateral tail vein (Figure 2F).
  - e. Secure tail vein tubing with a thin adhesive tape without touching the cannulation needle.
20. Place the mouse on a continuously heated MR cradle.
  - a. Connect the endotracheal tube to the MR compatible ventilation system supplying a rhythmic (80 breaths/min) delivery of a 20% O<sub>2</sub> to 80% air mixture with an isoflurane flow at 2%.
  - b. Set the ventilation system to a respiration cycle of 25% inhalation, 75% exhalation, and an inspiration volume of 1.8 mL/min.

△ **CRITICAL:** Ensure the breathing rate of the mouse is synchronized to the ventilation rhythm before proceeding.

21. Connect the tail vein tubing to the MR-compatible continuous infusion system.
  - a. Inject an initial bolus containing a mixture of pancuronium bromide (0.25 mg/kg) and medetomidine (0.05 mg/kg) for muscle relaxation and sedation, respectively.
  - b. Reduce isoflurane flow to 1.5% and set a timer to 5 min.

**Note:** Following the bolus injection, the breath-related motion should become significantly shallower within 20–30 sec.

△ **CRITICAL:** It is important to measure the systemic physiological parameters under anesthesia in a benchtop experiment that mimics the experimental conditions of the fMRI recordings. This to prevent any negative impact on the Blood Oxygenation Level Dependent (BOLD) fMRI signal that could result from anesthesia-related hyperoxia or hypercapnia. Our approach ensures a steady heart rate (measured in beats per minute, or bpm), pulse distension (measured in  $\mu\text{m}$ ), and oxygen saturation (measured in %) for at least one hour of anesthesia, as demonstrated in (Zerbi et al., 2019b).

22. Secure the animal's head within MR-compatible ear bars attached to the cradle (Figure 3).
  - a. Place an MR-compatible rectal probe to monitor a constant animal temperature of  $36 \pm 0.5^\circ\text{C}$  throughout scanning.
  - b. Connect the fiber patch cable to the optical fiber implant using a phosphor bronze mating sleeve.



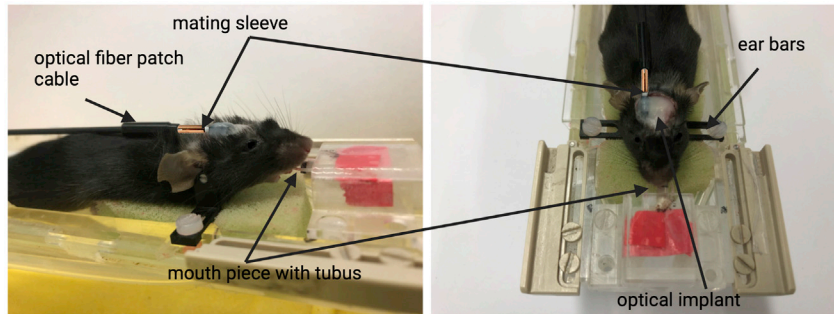


**Figure 3. Opto-fMRI cradle positioning and setup**

The intubation tubus of the mouse is connected to the mechanical ventilation machine through a small mouthpiece. Once breathing is confirmed to be synchronized to the ventilation rhythm, secure the mouse's head within the earbars and connect the fiber patch cable to the optical fiber using a phosphor bronze mating sleeve. Apply an artificial tear gel to both eyes to prevent drying.

**Note:** Choosing such an opaque, MR-compatible mating sleeve greatly reduces light spill at the fiber contact site compared to generic ceramic sleeves. This step should not re-position the animal's head within the ear bars.

- c. Apply an artificial tear gel to the animal's eyes to prevent drying.

**Optional:** Place an additional fiber patch cable beneath the animal's head for continuous illumination at the experimental stimulation wavelength throughout scanning. This measure will control for potential visual artifacts during optogenetic stimulation.

23. Reduce the isoflurane flow to 0.5% once the timer has expired and start a continuous infusion of medetomidine (0.1 mg/kg/h) and pancuronium bromide (0.4 mg/kg/h).
24. Insert the cradle into the MR bore equipped with the cryogenic probe, placing the animal's head at the center of the magnet.

**Optional:** As an additional light control measure, place an MR-compatible LED light source at the back of the MR cradle and switch it on. If installed, turn on the continuous laser emission of the control fiber path cable.

25. Run initial MR preparation scans suitable for your experimental design.

**Note:** This step may include measures to tune and match the frequency of the coil, adjustment for radiofrequency power, and standard adjustments to compensate for MR field inhomogeneities (e.g., MAPSHIM in a Bruker console).

**Optional:** Run a structural scan (T1-weighted or T2-weighted images) prior to functional data acquisition to assess correct optical fiber placement above the targeted regions and - if applicable - exclude animals that do not show correct targeting.

**△ CRITICAL:** Before functional data acquisition, ensure the laser system as well as the trigger program/device of choice is correctly set up to deliver precisely timed optogenetic stimuli.

**Alternatives:** This protocol uses the COSplay trigger device to precisely define, time, and deliver laser stimulation to the target brain region during fMRI recordings. Any other trigger device (e.g., Arduino) or software that can be coupled with the fMRI sequence can be used as well.

26. Start the desired sequence on the 7 Tesla Bruker PharmaScan scanner for functional data acquisition timed with the optogenetic trigger system.

**Note:** For BOLD fMRI recordings, we suggest using a gradient echo (GE) - echo planar imaging sequence (EPI) with a repetition time TR = 1000 ms, a slice thickness ST = 0.45 mm, and an in-plane spatial resolution RES = 0.22 × 0.2 mm<sup>2</sup>.

27. Switch off the continuous laser illumination and stop the delivery of isoflurane as well as the continuous infusion of the anesthesia mixture after the functional recordings.

**Note:** Routinely check on the animal connected to the ventilation machine until the muscle relaxant pancuronium bromide is metabolized. When this occurs, the animal will start counter-breathing, attempt small movements, and try to detach itself from the intubation line.

**△ CRITICAL:** Remove the intubation tube from the mouse trachea only when you are confident that the animal can breathe autonomously. Inject up to 1 mL of saline solution subcutaneously to rehydrate the mouse and put it in a heated chamber to fully recover from the anesthesia. Regularly check the breathing of the animal.

### EXPECTED OUTCOMES

Combining optogenetic stimulation with BOLD fMRI recordings reliably captures both local and remote signals across the mouse brain. Due to the high spatial and temporal precision of optogenetics, this multimodal approach creates a unique scenario where obtained brain-wide activation patterns can be causally explained. Once successfully implemented, opto-fMRI can visualize the dynamic nature of brain activity traveling through complex circuits while extending the interpretability of fMRI data by defining cell type-specific contributions to the BOLD signal.

Except for the optic fiber cannula, the implant does not create strong MR artifacts, nor does it limit local BOLD detection if the recommended materials are used, and the experimental and analytical recommendations are followed (Figure 4A). However, incompatible dental cement can lead to increased distortions along the anterior-posterior axis (Figure 4B). Furthermore, the described surgical procedure will result in a stable optical implant that is suitable for longitudinal studies with repeated measurements.

Visual artifacts due to laser light emission in the otherwise dark environment of an MR scanner can be a potential confounding factor and result in co-activation of the visual system. However, by continuously illuminating the inside of the MR scanner and adding an additional laser light source emitting at the experimental wavelength, transient optogenetic stimulation pulses should not evoke a visual response. Following this set-up, no BOLD activity in visual association areas of experimental animals nor control animals which received laser stimulation but did not express the optogenetic actuator ChR2 (*data not shown*) was captured (Figure 4C). An example of visual artifacts due to insufficient MR illumination / lack of a continuous, wavelength-matched laser light emitting source is given in Figure 4D.

### QUANTIFICATION AND STATISTICAL ANALYSIS

Our protocol for data analysis uses in-house MATLAB scripts and the software packages FSL (FMRIB Software Library, UK) and AFNI (Analysis of Functional NeuroImages, USA) to preprocess and analyze the functional data. Each scanning session is stored in a separate folder containing the individual adjustment files as well as the raw structural and functional datasets.

1. Import folders and convert the contained files from the MR output format (e.g., Bruker) to Analyze format using a suitable converter (e.g., dicomifier, pvconv.pl).

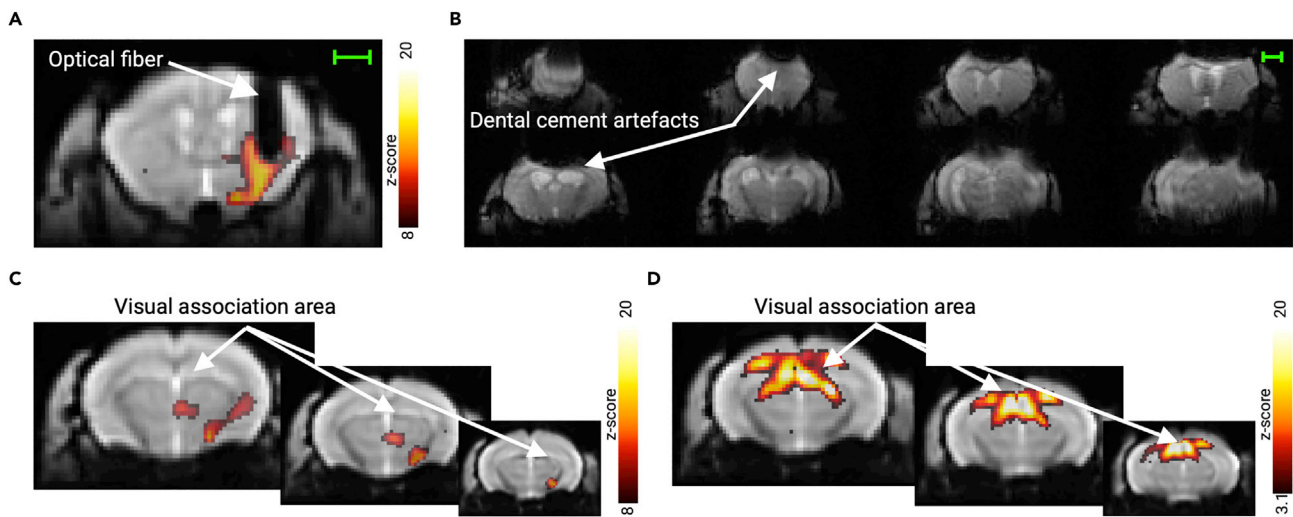


**Figure 4. Quality of opto-fMRI datasets**

(A) Susceptibility artifact of the optical fiber and local BOLD detection.

(B) MR artifacts due to MR-incompatible dental composite.

(C) With appropriate light controls, no BOLD signal is detectable in visual association areas.

(D) Without appropriate light controls, strong BOLD signals are elicited in visual association areas. Scale bars represent 1 mm.

- In MATLAB, increase the voxel size to guarantee compatibility of the acquired mouse data with the commonly used human fMRI data analysis toolboxes. We recommend loading the header information of each dataset with the Matlab toolbox 'Tools for NIfTI and ANALYZE image' using the command.

```
>load_untouch_header_only([headername, '.hdr']);
```

and multiplying the current voxel dimensions by 10.

△ **CRITICAL:** While regular human MR scanner systems operate in seconds, the Bruker system utilized for this study uses millisecond timescales. We recommend checking the header information of functional datasets with regards to the correct repetition time (TR) and adjust if necessary, using e.g.,

```
>fsledithd your_func_data.nii.gz
```

- Further pre-processing of the data and subsequent, single-subject GLM-based analysis are performed via the FSL FEAT pipeline. A detailed manual for FSL FEAT is available at <https://fsl.fmrib.ox.ac.uk/fsl/fslwiki/FEAT/UserGuide>.
  - Load the functional datasets and select the desired options in the 'Pre-stats' rider. We recommend selecting the implemented MCFLIRT motion correction option, spatial smoothing, and temporal filtering using a highpass filter estimated from the input data. Instead, options like BET brain extraction and slice timing correction are discouraged when handling functional data from rodents as they may lead to sub-optimal segmentation of the brain and errors in the registrations.

△ **CRITICAL:** When normalizing the data in a common template for opto-fMRI statistical analyses, we strongly recommend creating a study-specific EPI and/or structural template that accounts for the field distortions from the optical fiber (Figure 5A). For this, 10–15 datasets are usually taken and used to generate a study specific template, e.g., in ANTs:

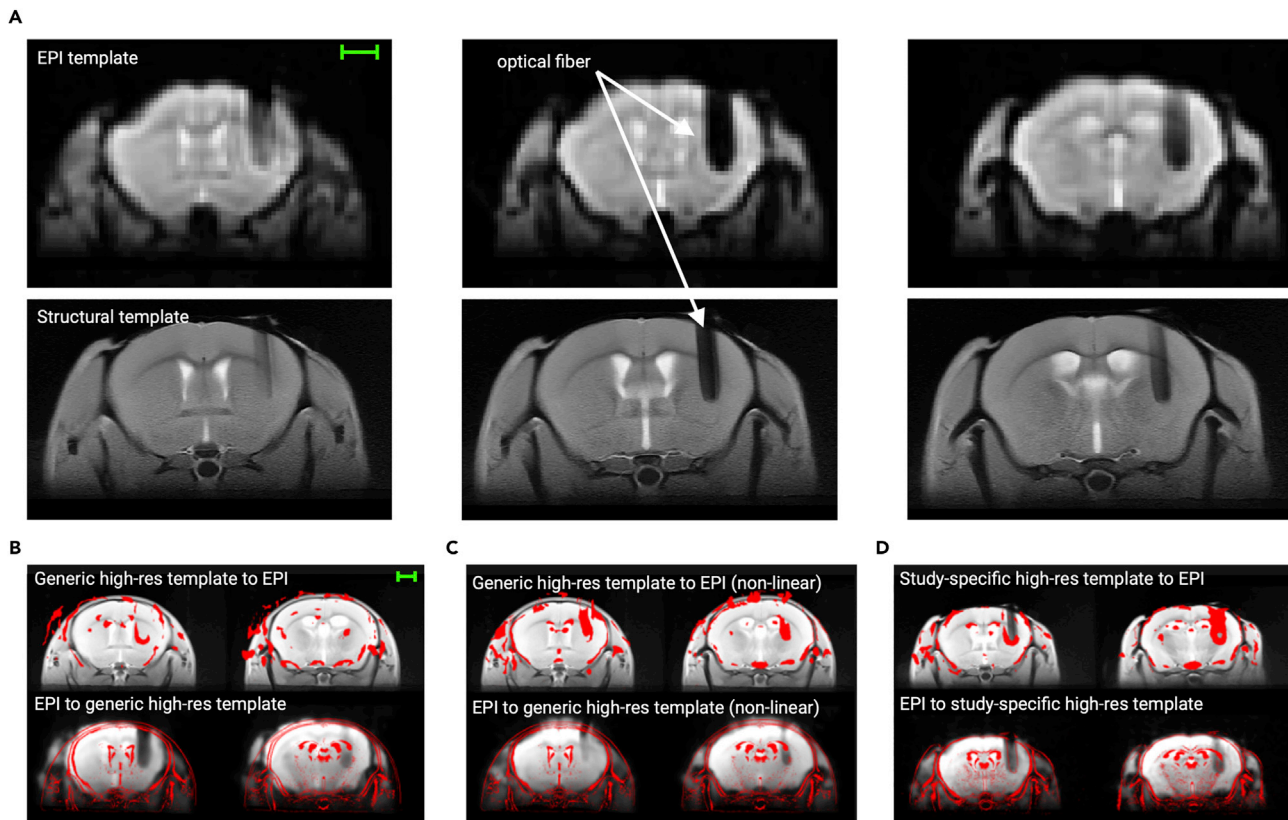


**Figure 5. Registration of opto-fMRI datasets**

(A) Creating a study-specific EPI and/or T1/T2-weighted structural template accounts for the field distortions caused by the optical fiber.  
 (B) Using a generic mouse brain template for opto-fMRI datasets can result in insufficient normalization.  
 (C) Non-linear transformation parameters can cause warping around the optical fiber and thus, hinder correct BOLD signal detection.  
 (D) A study-specific standard space template and a linear transform will properly account for the placement (and susceptibility artifacts) of the optical fiber. Scale bars represent 1 mm.

```
>buildtemplateparallel.sh -d ImageDimension -o YourEPItemplate_ <other options> <YourEPIImages.nii.gz or YourStructuralImages.nii.gz>;
```

Immediately normalizing datasets to a generic mouse brain template without fiber placement can for example result in an insufficient fit around the perimeter of the brain (Figure 5B). Additionally, the type of transformation to go from EPI to a generic template space can introduce distortions in datasets with an optical fiber. Panel C shows how a non-linear rather than linear transformation causes significant warping and zooming around the optical fiber. Instead, registering the EPI dataset to a study-specific template first by means of a linear transform maintains a correct representation of the optical fiber (Figure 5D) and ultimately greatly assists in normalizing the functional data to the generic high-resolution standard space template.

- b. In the 'Stats' rider, select FILM prewhitening and FSL's standard motion parameters for motion regression and set up the GLM using the 'Full model setup' option. This step requires you to define the optogenetic stimulation protocol used during the functional scan acquisition in a 3-column format as well as the hemodynamic response function that will be convolved with the stimulation design. We recommend testing appropriate HRF functions that best match to your BOLD responses elicited under the optic fiber. Adding the temporal derivative will also account for potentially delayed responses upon the optogenetic stimulation. In the 'Contrasts & F-tests' rider set up the desired contrasts.
- c. In the 'Post-stats' rider, define the desired thresholding method.

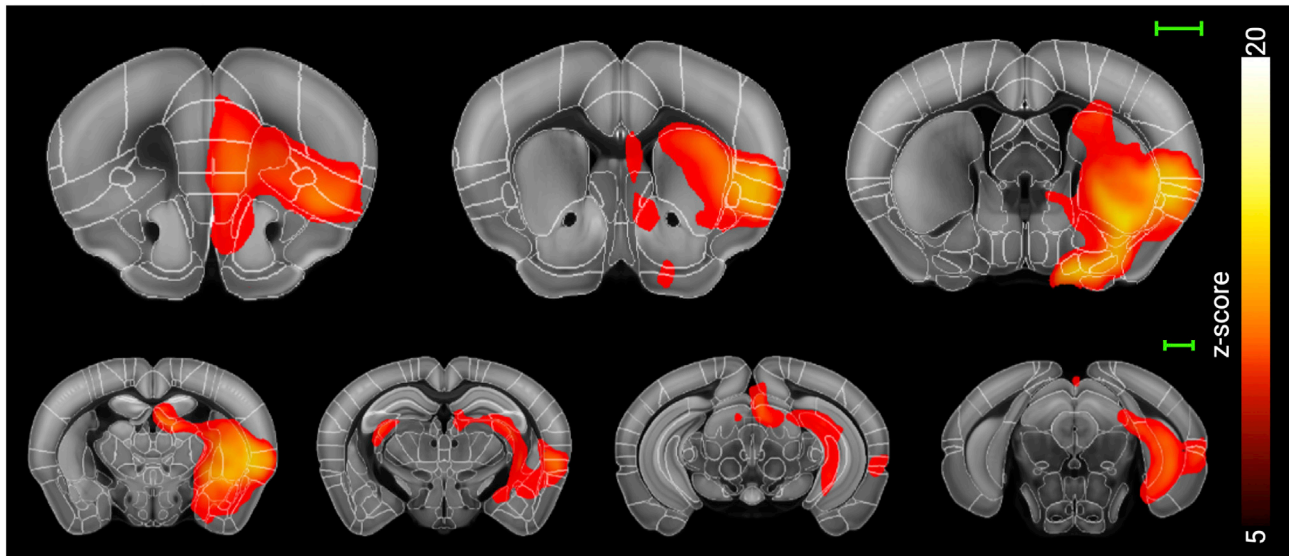


**Figure 6. Group statistical parametric map in high-resolution standard space**

Scale bars represent 1 mm.

- d. Press 'Go' to run first-level (single-subject) GLM analysis.
4. Once first-level analysis is finished, assess the registration quality for every subject and re-run first-level analysis with adjusted registration parameters if necessary.
5. Assess statistical parametric maps of individual datasets. In case of subjects that do not show significant activation clusters, we recommend to cross-validate them with their respective histological stainings of the viral transfection. This will aid in correctly identifying non-responders that must be included in all analyses and animals that can be excluded due to unsuccessful viral transfection.
6. Having designed your GLM matrix for group-level statistical comparisons, run higher level (group-level) analysis using FSL's lower-level FEAT directories as inputs to obtain statistical group activation maps (Figure 6).

## LIMITATIONS

This protocol describes opto-fMRI data acquisition using a high signal-to-noise ratio (SNR) cryogenic coil set-up. However, such a resource might not be available to the experimenter. Using other commercially available or home-made MR surface coils, we cannot guarantee comparable dataset quality in terms of spatial resolution throughout the depth of the brain tissue. Furthermore, depending on the experimental question, the optogenetic stimulation parameters might require higher light intensities than described here. Under such circumstances, optogenetic illumination has been shown to cause photodilation of the local vasculature independent of neural activity (Rungta et al., 2017). Thus, the implementation of appropriate control experiments is critical to account for potential spurious BOLD signals.

## TROUBLESHOOTING

### Problem 1

Optical fiber cladding does not lay flat on the skull surface (step 10).

### Potential solution

Consider implanting the optical fiber at an angle to avoid aereous space between skull surface and optical fiber cladding.

### **Problem 2**

Abrasion of optical fiber cladding over time, resulting in loss of optical fiber laser light transmission (step 13).

### **Potential solution**

Ensure the cladding is sufficiently covered in dental cement without excessively increasing the height of the implant.

### **Problem 3**

Optical implant is loose/falls off (step 11).

### **Potential solution**

Make sure all connective tissue is removed, no active bleeding is present, and the skull surface is dry before applying the dental bonding agent. Consider the use of plastic/titanium screws on the skull surface if the problem persists.

### **Problem 4**

Optical fiber and fiber patch cable do not connect seamlessly (step 12).

### **Potential solution**

Ensure no dental cement is transferred onto the ceramic ferrule of the optical fiber.

### **Problem 5**

Optogenetic stimulation does not start (step 26).

### **Potential solution**

Ensure the trigger output of the MRI is connected to the input of the laser setup. Check the 'Trigger Out' checkbox in ParaVision for your EPI scan.

### **Problem 6**

Functional MR images show strong susceptibility artifacts around the optical fiber and the optical implant.

### **Potential solution**

Slowly insert the optical fiber into the brain to avoid excessive tissue rupture and bleeding. Ensure no air bubbles or clotted blood is trapped beneath the dental cement. When using a different MR setup, check compatibility of materials a phantom first.

## **RESOURCE AVAILABILITY**

### **Lead contact**

Further information and requests for resources and reagents should be directed to and will be fulfilled by the lead contact, Valerio Zerbi ([valerio.zerbi@epfl.ch](mailto:valerio.zerbi@epfl.ch)).

### **Materials availability**

This study did not generate new unique reagents.

### **Data and code availability**

Original data have been deposited to zenodo.org: <https://doi.org/10.5281/zenodo.6770220>.

## **ACKNOWLEDGMENTS**

C.G. and V.Z. are supported by the research grant ETH 062-18 and the Swiss National Science Foundation (SNSF) AMBIZIONE (PZ00P3\_173984/1) and ECCELLENZA (PCEFP3\_203005). The authors



would like to thank Dr. Giovanna Ielacqua for the images of mouse intubation and tail vein cannulation.

## AUTHOR CONTRIBUTIONS

Conceptualization, methodology, and investigation, C.G. and V.Z.; writing – original draft, C.G.; writing – review and editing, C.G., N.W., and V.Z.; funding acquisition, V.Z.; supervision, V.Z.

## DECLARATION OF INTERESTS

The authors declare no competing interests.

## REFERENCES

- Avants, B.B., Tustison, N.J., Song, G., Cook, P.A., Klein, A., and Gee, J.C. (2011). A reproducible evaluation of ANTs similarity metric performance in brain image registration. *Neuroimage* 54, 2033–2044. <https://doi.org/10.1016/j.neuroimage.2010.09.025>.
- Avants, B.B., Yushkevich, P., Pluta, J., Minkoff, D., Korczykowski, M., Detre, J., and Gee, J.C. (2010). The optimal template effect in hippocampus studies of diseased populations. *Neuroimage* 49, 2457–2466. <https://doi.org/10.1016/j.neuroimage.2009.09.062>.
- Aymanns, F., Rudin, M., and Ioannas, H.-I. (2020). COSplay: contrast optimized stimulation player. *J. Open Source Softw.* 4, 1171. <https://doi.org/10.21105/joss.01171>.
- Das, S., MacDonald, K., Chang, H.Y.S., and Mitzner, W. (2013). A simple method of mouse lung intubation. *J. Vis. Exp.* e50318 <https://doi.org/10.3791/50318>.
- Frässle, S., Aponte, E.A., Bollmann, S., Brodersen, K.H., Do, C.T., Harrison, O.K., Harrison, S.J., Heinzle, J., Iglesias, S., Kasper, L., et al. (2021). TAPAS: an open-source software package for translational neuromodeling and computational psychiatry. *Front. Psychiatry* 12, 680811. <https://doi.org/10.3389/fpsy.2021.680811>.
- Gong, S., Doughty, M., Harbaugh, C.R., Cummins, A., Hatten, M.E., Heintz, N., and Gerfen, C.R. (2007). Targeting Cre recombinase to specific neuron populations with bacterial artificial chromosome constructs. *J. Neurosci.* 27, 9817–9823. <https://doi.org/10.1523/JNEUROSCI.2707-07.2007>.
- Grandjean, J., Canella, C., Anckaerts, C., Ayranci, G., Bougacha, S., Bienert, T., Buehlmann, D., Coletta, L., Gallino, D., Gass, N., et al. (2020). Common functional networks in the mouse brain revealed by multi-centre resting-state fMRI analysis. *Neuroimage* 205, 116278. <https://doi.org/10.1016/j.neuroimage.2019.116278>.
- Grimm, C., Duss, S.N., Privitera, M., Munn, B.R., Frässle, S., Chernysheva, M., Patriarchi, T., Razansky, D., Wenderoth, N., Shine, J.M., et al. (2022). Locus Coeruleus firing patterns selectively modulate brain activity and dynamics. *bioRxiv*. <https://doi.org/10.1101/2022.08.29.505672>.
- Grimm, C., Frässle, S., Steger, C., von Ziegler, L., Sturman, O., Shemesh, N., Peleg-Raibstein, D., Burdakov, D., Bohacek, J., Stephan, K.E., et al. (2021). Optogenetic activation of striatal D1R and D2R cells differentially engages downstream connected areas beyond the basal ganglia. *Cell Rep.* 37, 110161. <https://doi.org/10.1016/j.celrep.2021.110161>.
- Markicevic, M., Fulcher, B., Lewis, C., Helmchen, F., Rudin, M., Zerbi, V., and Wenderoth, N. (2020). Cortical excitation:inhibition imbalance causes abnormal brain network dynamics as observed in neurodevelopmental disorders. *Cereb. Cortex* 30, 4922–4937. <https://doi.org/10.1093/cercor/bhaa084>.
- Oh, S.W., Harris, J.A., Ng, L., Winslow, B., Cain, N., Mihalas, S., Wang, Q., Lau, C., Kuan, L., Henry, A.M., et al. (2014). A mesoscale connectome of the mouse brain. *Nature* 508, 207–214. <https://doi.org/10.1038/nature13186>.
- Rungta, R.L., Osmanski, B.F., Boido, D., Tanter, M., and Charpak, S. (2017). Light controls cerebral blood flow in naive animals. *Nat. Commun.* 8, 14191. <https://doi.org/10.1038/ncomms14191>.
- Zerbi, V., Floriou-Servou, A., Markicevic, M., Vermeiren, Y., Sturman, O., Privitera, M., von Ziegler, L., Ferrari, K.D., Weber, B., De Deyn, P.P., et al. (2019a). Rapid reconfiguration of the functional connectome after chemogenetic locus coeruleus activation. *Neuron* 103, 702–718.e5. <https://doi.org/10.1016/j.neuron.2019.05.034>.
- Zerbi, V., Grandjean, J., Rudin, M., and Wenderoth, N. (2015). Mapping the mouse brain with rs-fMRI: an optimized pipeline for functional network identification. *Neuroimage* 123, 11–21. <https://doi.org/10.1016/j.neuroimage.2015.07.090>.
- Zerbi, V., Ielacqua, G., Markicevic, M., Haberl, M., Ellisman, M., A-Bhaskaran, A., Frick, A., Rudin, M., and Wenderoth, N. (2018). Dysfunctional autism risk genes cause circuit-specific connectivity deficits with distinct developmental trajectories. *Cereb. Cortex* 28, 2495–2506. <https://doi.org/10.1093/cercor/bhy046>.
- Zerbi, V., Markicevic, M., Gasparini, F., Schroeter, A., Rudin, M., and Wenderoth, N. (2019b). Inhibiting mGluR5 activity by AFQ056/Mavoglurant rescues circuit-specific functional connectivity in Fmr1 knockout mice. *Neuroimage* 191, 392–402. <https://doi.org/10.1016/j.neuroimage.2019.02.051>.